IgA-driven neutrophil activation underlies post-Zika severe dengue disease in humans

Authors:

Jaime A. Cardona-Ospina[1,2], Vicky Roy[3], Dorca E. Marcano-Jiménez[4], Sandra Bos[1], Elias Duarte[1], José V. Zambrana[5,6], Agamjot Bal[1], Antonio Gregorio Dias Jr.[1], Julia Zhiteneva[3], Julia Huffaker[1], Carlos Montenegro[5], Guillermina Kuan[5,7], Marcos J. Ramos-Benitez[4], Angel Balmaseda[5,8], Galit Alter[3], Eva Harris[1]*

Affiliations:

[1]Division of Infectious Diseases and Vaccinology, School of Public Health, University of California, Berkeley, Berkeley, CA

[2]Grupo Biomedicina, Facultad de Medicina, Institución Universitaria Visión de las Américas, Pereira, Colombia

[3]Ragon Institute of MGH, MIT, and Harvard, Cambridge, MA

[4]Department of Basic Sciences, Ponce Health Sciences University and Ponce Research Institute, Ponce, Puerto Rico

[5]Sustainable Sciences Institute, Managua, Nicaragua

[6]Department of Epidemiology, School of Public Health, University of Michigan, Ann Arbor, MI

[7]Centro de Salud Sócrates Flores Vivas, Ministerio de Salud, Managua, Nicaragua

[8]Laboratorio Nacional de Virología, Centro Nacional de Diagnóstico y Referencia, Ministerio de Salud, Managua, Nicaragua

*Corresponding author. Email: eharris@berkeley.edu

Abstract

The four dengue virus serotypes (DENV1-4) and the related Zika flavivirus (ZIKV) are major public health concerns worldwide. Primary immunity against ZIKV increases the risk of a subsequent severe DENV2 infection, presenting a significant challenge for developing safe and effective ZIKV vaccines. However, the mechanisms driving this phenomenon remain unclear. Leveraging our long-standing Pediatric Dengue Cohort Study in Nicaragua, we show that serum anti-NS1 IgA antibodies elicited after a primary ZIKV infection drive neutrophil activation and correlate with increased risk of subsequent severe DENV2 disease. Depletion experiments combined with e*x vivo* functional NETosis assays confirmed that anti-NS1 IgA antibodies drive neutrophil activation in dengue hemorrhagic fever/dengue shock syndrome (DHF/DSS). Moreover, increased neutrophil degranulation in paired serum samples obtained during the acute DENV2 infection from the same individuals correlated with IgA binding to DENV2 NS1 and preceded the development of vascular leakage. This finding was corroborated in an orthogonal hospital-based study. Thus, serum anti-NS1 IgA enhances neutrophil activation in severe dengue, with implications for prognostics, therapeutics, and vaccines.

Main Text

The four serotypes of dengue virus (DENV1-4) and Zika virus (ZIKV) are closely related flaviviruses that co-circulate and constitute the most prevalent causes of arboviral disease globally [1]. DENV infections exhibit a clinical spectrum ranging from a self-limited febrile illness (dengue fever [DF]) to more severe, potentially fatal forms such as dengue hemorrhagic fever and dengue shock syndrome (DHF/DSS) characterized by thrombocytopenia, vascular leakage, and hemorrhagic manifestations[2]. Sequential infections with different DENV serotypes or ZIKV can either confer protection or increase the risk of subsequent severe disease[3–5]. This phenomenon, primarily driven by the humoral immune response, presents significant challenges for the development of safe and effective vaccines.

During sequential DENV infections, sub-neutralizing cross-reactive IgG antibodies targeting structural viral proteins can facilitate viral entry into myeloid cells expressing Fcγ receptors, increasing viral load through a phenomenon known as antibody-dependent enhancement (ADE)[6,7]. In addition, afucosylated IgG antibodies generated during the acute secondary infection further enhance disease severity by promoting cellular activation via FcγRIIIA[8,9]. Epidemiological studies have shown that a primary ZIKV infection increases the likelihood of subsequent symptomatic DENV infections and severe disease[4,5]. This association is strongly correlated with antibody levels, as a specific range of ZIKV-induced DENV cross-reactive antibodies are linked to an elevated risk of severe outcomes upon a subsequent DENV infection[4]. Therefore, understanding the antibody features that underlie this increased risk is essential for developing safe and effective vaccines.

To explore this, we employed an agnostic systems serology approach to characterize DENV cross-reactive antibodies after a prior ZIKV infection and before a subsequent symptomatic infection with DENV2, leveraging unique serum samples from our long-standing Pediatric Dengue Cohort Study (PDCS) in Nicaragua[10]. Our findings reveal that pre-existing IgA antibodies, particularly those targeting the nonstructural protein 1 (NS1), are key predictive features of DHF/DSS. Using systems serology and functional assays in paired pre-infection and acute-phase samples from the same individuals, we provide novel insights into the role of anti-NS1 IgA antibodies in mediating heightened neutrophil activation, a characteristic of children that progressed to severe disease. This insight reveals a previously unappreciated mechanism of IgA-mediated neutrophil activation in dengue disease that may underpin progression to severe disease

in sequential flavivirus infections. These results have broad implications for understanding immune responses against flaviviruses in co-endemic regions and informing vaccine development. Moreover, they highlight the potential role of serum IgA antibodies in mediating neutrophil-mediated pathogenesis in infectious diseases.

Results

Pre-existing IgA antibodies differentiate severe and non-severe DENV infections

A prior ZIKV infection increases the risk of both symptomatic and severe disease during a subsequent DENV infection[4,5,11]. While this elevated risk has been linked to DENV cross-reactive antibodies induced by ZIKV[4], the specific characteristics of these antibodies remain undefined. To address this gap, we employed an agnostic systems serology approach to evaluate the antigenic targets and isotypes of pre-existing antibodies associated with increased risk of DHF/DSS.

Our analysis focused initially on serum samples collected after primary ZIKV infection and before subsequent DENV2 infection from 24 children enrolled in the PDCS in Nicaragua. These children experienced a primary ZIKV infection in 2016, followed by a DENV2 infection in 2019–2020, which resulted in either DF (n = 14) or DHF/DSS (n = 10; Fig. 1A). Using a multiplexed bead-based assay[12], we characterized the antibody binding profile against the envelope protein (E), domain III of E (EDIII), and NS1 of DENV1–4 and ZIKV, evaluating total IgG, IgG1–4, IgM, and IgA antibodies.

After correcting for false discovery rate (FDR), only binding of IgA antibodies differed significantly between the clinical groups across all tested antigens and isotypes (fig. S1A). Additionally, increased ED_{50} values of IgA antibodies, reflecting the dilution at which binding is reduced to 50%, were uniquely associated with an elevated risk of developing DHF/DSS (Fig. 1B). In a regularized multivariate model, IgA binding to NS1 of the incoming serotype (DENV2) emerged as the variable with the highest adjusted coefficient, highlighting its strong association with severe disease outcomes (Fig. 1C).

To corroborate the discriminative potential of IgA binding suggested by the ED_{50} analysis, we assessed avidity by measuring antibody binding in the presence of urea as a chaotropic agent using our multiplexed bead-based assay[13]. We compared the predictive performance for the development of DHF/DSS of IgA and IgG avidity. Notably, IgA avidity alone predicted DHF/DSS

with an accuracy of 92% (95% CI: 62%–99%, p = 0.014; Fig. 1D), while IgG avidity neither predicted outcomes nor enhanced the model's performance (fig. S1B).

These findings established pre-existing high-avidity IgA antibodies induced after a primary ZIKV infection as key discriminative features associated with the development of DHF/DSS during a subsequent DENV2 infection.

Pre-existing anti-NS1 IgA antibodies drive neutrophil effector functions *ex vivo* in children who developed DHF/DSS

Although IgA antibodies have been mainly studied in the context of mucosal immunity, they constitute the second most abundant immunoglobulin isotype in human serum, following IgG1[14,15]. Neutrophils are the primary and most abundant effectors of IgA antibodies[16]. Notably, IgA-mediated neutrophil activation is thought to contribute to the pathogenesis of IgA-mediated immune diseases through formation of IgA-immune complexes[17]. Several IgA-mediated immune diseases share clinical features with DHF/DSS, such as thrombocytopenia, arthralgia, petechiae and kidney involvement[18]. Considering this, we investigated whether pre-existing IgA antibodies could enhance neutrophil effector functions and be associated with the development of severe dengue disease.

To evaluate whether pre-existing antibodies influence neutrophil activation, we evaluated antibody-dependent neutrophil effector functions in *ex vivo* functional assays. Considering that phagocytosis and NETosis are key neutrophil effector functions[19], we implemented *ex vivo* functional assays to measure antibody-dependent neutrophil phagocytosis (ADNP) and NETosis as a readout of antibody-dependent neutrophil activation. For ADNP, beads were coupled with either E or NS1 from the incoming serotype (DENV2). They were opsonized with the pre-infection serum of the participants and used to assess neutrophil phagocytosis of the beads via flow cytometry[20]. Our results revealed that children who subsequently developed thrombocytopenia exhibited significantly higher ADNP against NS1 compared to those who did not (fig. S2A). In fact, ADNP against NS1 consistently exceeded ADNP against E across different clinical endpoints (fig. S2A). This observation prompted a within-group comparison of ADNP responses to NS1 and E. We found that the serum from children who developed DHF/DSS or displayed hallmarks of severe disease consistently induced higher ADNP against NS1 than to E (Fig. 2A).

Considering this observation and given that IgA antibodies against DENV2 NS1 showed the highest adjusted coefficient in our multivariate model of antibody binding, we sought to determine whether the antibody-dependent neutrophil effector functions induced by pre-existing antibodies were specifically driven by IgA and targeted against NS1. To do this, we employed a complementary experimental approach. Due to the technical challenges of purifying IgA from small serum volumes, we compared the ability of IgA-depleted and mock-depleted serum to induce NETosis in an *ex-vivo* functional assay[21]. In this assay, wells coated with either E or NS1 were incubated with IgA-depleted or mock-depleted pre-infection serum, and the induction of neutrophil extracellular traps (NETs) was quantified using a fluorescence-based assay. Importantly, in the absence of antibodies, E and NS1 induced minimal NET formation (fig. S2B). However, NS1 induced robust NETosis in the presence of IgA, and depleting IgA from the serum of children who developed DHF/DSS almost completely abrogated NET formation in response to NS1 (Fig. 2, B and D). In contrast, IgA depletion had no effect on NETosis induction in response to E (Fig. 2, B and C).

All together, these results demonstrate that pre-existing antibodies, particularly IgA targeting NS1, play a critical role in driving neutrophil effector functions, as evidenced by ADNP and NETosis in *ex vivo* functional assays.

Post-ZIKV severe DENV infections are characterized by enhanced neutrophil activation in acute-phase sera correlating with IgA binding to NS1

Consequently, we evaluated neutrophil involvement during the subsequent acute DENV2 infection in participants who progressed to DHF/DSS. To do this, we assessed serum samples obtained during the acute DENV2 infection of the same 24 participants (DF=14, DHF/DSS=10) from the PDCS. Initially, we evaluated circulating neutrophil levels during acute infection. On day three post-fever onset, just before the emergence of severe disease, children who progressed to DHF/DSS exhibited significantly higher relative neutrophil counts compared to those who developed DF (Fig. 3, A and B).

Next, we examined neutrophil degranulation, a key neutrophil effector function measurable in serum. We analyzed levels of components of primary granules (myeloperoxidase [MPO], neutrophil elastase [NE]), secondary granules (lactoferrin [LF]), and tertiary granules (matrix

metalloproteinase 9 [MMP-9]) in serum collected on days 1-3 post-fever onset (Table S1). Importantly, primary granule components were significantly elevated in children with DHF/DSS and were associated with heightened risk of developing severe clinical manifestations, including mucosal bleeding, vascular leakage, and increased risk of ICU admission (Fig. 3, C and D).

Thereafter, we evaluated whether this enhanced neutrophil degranulation was correlated with antibody binding. In agreement with our experimental observation and statistical prediction in pre-infection samples, IgA binding to NS1 positively correlated with levels of primary granule components, while IgG antibodies correlated negatively with degranulation markers (Fig. 3E). This highlights a distinct association between IgA antibodies targeting NS1 and heightened neutrophil activation early in the evolution to severe disease.

In this study, analysis of DENV2 viral loads during acute infection revealed no significant differences between clinical groups at the time of assessment (early post-fever onset; Fig. 3C), a finding also observed in post-ZIKV DENV infections in a different population in Brazil[11].

These findings corroborate our experimental observations in pre-infection samples and *ex vivo* functional assays and demonstrate that severe post-ZIKV DENV infections are characterized by increased neutrophil activation that correlates with IgA antibodies in serum binding to NS1. Furthermore, these results highlight serum IgA antibodies directed against NS1 as key drivers of enhanced neutrophil activation during acute DENV2 infection.

Enhanced neutrophil activation precedes the development of vascular leakage and progression to DHF/DSS

To validate our findings, we investigated neutrophil involvement in the Pediatric Dengue Hospital-based Study (PDHS), an independent study conducted in Managua, Nicaragua. This study enrolls participants under 15 years of age presenting with acute febrile illness suspected of dengue; DENV infections are laboratory-confirmed and serotyped by RT-PCR[22]. We screened children in the PDHS with DENV2 infections during the 2018–2020 epidemic to identify those with prior ZIKV exposure using our serotyping approach[4,12].

A total of 111 dengue cases with past ZIKV infections were identified (DF=67, DHF/DSS=44). Consistent with the PDCS observations, children who developed DHF/DSS exhibited significantly higher neutrophil counts compared to those with DF prior to progression to

DHF/DSS (Fig. 4A and fig. S3A). We further explored neutrophil activation in a subset of samples (18 DHF/DSS and 36 DF cases) collected early after fever onset (≤3 days post fever onset), matched for age and sex. As in prior analyses, significantly elevated markers of neutrophil degranulation, particularly MPO and NE components of primary granules, were observed in individuals who progressed to DHF/DSS (Fig. 4B).

Finally, we investigated whether neutrophil degranulation preceded the development of vascular leakage, a defining feature of DHF/DSS. To address this, we used gallbladder wall thickness as a quantitative marker of vascular leakage[23–25]. Gallbladder wall edema, a result of vascular leakage, is observed as DENV infection progresses to severe disease (Fig. 4C). This ultrasonographic metric provides a robust, continuous measure that is unaffected by treatment interventions and is widely and consistently employed in our setting for clinical triage and follow-up [23]. We found that the maximum gallbladder wall thickness – typically reached on day 4 post-fever onset or later (Fig. 4C) – was positively correlated with levels of primary granule components measured on day 3 or earlier in both PDCS and PDHS participants (Fig. 4, D and E). These findings reveal that neutrophil activation precedes vascular leakage, implicating a role in the pathogenesis of severe dengue disease.

Discussion

The introduction of ZIKV into endemic regions of Latin America resulted in the widespread co-circulation of ZIKV and the closely related flaviviruses, DENV1-4. ZIKV continues to circulate at low levels in Asia alongside the four DENV serotypes[26]. Like sequential DENV infections with different serotypes, prior ZIKV immunity increases the risk of subsequent severe dengue disease [4,5]. However, we and others found that post-ZIKV DENV infections that progress to severe disease do not exhibit the elevated viral load associated with antibody-enhanced DENV infections[11]. This suggests that alternative immune mechanisms may contribute to the heightened risk of severe disease in these cases. Therefore, we performed an agnostic serological analysis of potential biomarkers correlated with the risk of subsequent severe dengue disease. Surprisingly, serum IgA antibodies were key discriminative features between clinical groups. Then, we focused on serum IgA, an often-overlooked antibody isotype in immune responses to infectious diseases. Our findings demonstrate that serum IgA antibodies targeting NS1 drive neutrophil activation in severe post-ZIKV dengue disease. Importantly, we establish a temporal relationship between pre-existing

anti-NS1 IgA antibodies and heightened neutrophil activation during acute infection. In addition, we show that this increased neutrophil activation not only precedes but also correlates with the development of vascular leakage – a critical hallmark of severe dengue disease.

IgA antibodies in human serum are present at concentrations comparable to IgG3 and IgG2[14,15]. Although extensively studied in mucosal immunity, the role of IgA antibodies in human serum – whether protective or pathogenic – has been largely overlooked. This gap partly reflects limitations in mouse models, which naturally lack CD89 (Fc alpha receptor), a critical receptor for IgA on human myeloid cells[27]. Of note, elevated IgA immune complexes have been implicated in autoimmune diseases through neutrophil activation; these diseases share clinical features with dengue, such as rash, petechiae, thrombocytopenia, and kidney involvement[17,18,28]. In the context of infectious diseases, serum IgA antibodies can mediate virus neutralization[29], and DENV IgA antibodies targeting structural components can block ADE and neutralize the virion[30]. In contrast, our study demonstrates that IgA antibodies against NS1, a non-structural protein that is secreted during infection, induce neutrophil activation in DHF/DSS preceding vascular leakage. While previous studies have reported DENV-associated IgA nephropathy and elevated titers of IgA in children with DHF/DSS[31,32], the absence of a temporal relationship between IgA responses and disease progression has hindered understanding of its role in DENV pathogenesis. By analyzing samples collected after primary ZIKV infection and prior to subsequent DENV2 infection, we establish a temporal link between pre-existing ZIKV-induced IgA antibodies targeting DENV NS1, heightened neutrophil activation, and progression to DHF/DSS.

Importantly, heightened neutrophil activation has consistently been associated with severe dengue disease in humans[33–35]. Indeed, genes associated with increased neutrophil functions have been proposed as prognostic markers of severe dengue[36,37] Nevertheless, the link between neutrophil activation and pre-existing antibodies, a major risk factor for DHF/DSS, has remained elusive. Interestingly, DENV induces the production of immature neutrophils[38], which predominantly synthesize primary granules containing MPO and NE, degranulation markers associated with DHF/DSS. In parallel, serum IgA, to a greater extent than IgG, has been shown to enhance neutrophil effector functions during viral infections[39,40]. Based on these observations and our results, we hypothesize that IgA/NS1 immune complexes drive heightened activation of immature neutrophils during infection, contributing to vascular dysfunction and organ damage. The pathogenic role of neutrophil activation has been well-documented in other infectious

diseases, such as malaria and leishmaniasis[41,42]. Although the current understanding of DHF/DSS immunopathogenesis is centered on the role of IgG antibodies targeting structural components of the virion in the context of ADE[8,9], we believe that enhanced neutrophil activation due to cross-reactive anti-NS1 IgA antibodies may contribute to disease pathogenesis in sequential DENV infections.

Nonetheless, our study has several limitations. Existing murine DENV disease models lack expression of the Fc alpha receptor (CD89) and exhibit IgA immunobiology distinct from humans[27]. This limited our ability to validate IgA-mediated neutrophil activation as a direct cause of vascular leakage and severe disease. Instead, we conducted *ex vivo* functional assays using primary cells from healthy human donors, which demonstrated a strong association between IgA antibodies targeting NS1, neutrophil activation, and severe disease. We showed that IgA depletion in the presence of NS1 but not E significantly reduced neutrophil effector functions, underscoring the specificity of this response. On the other hand, although our findings suggest distinct roles for IgA antibodies targeting NS1 versus structural components such as E, the mechanisms underlying their differential contributions to neutrophil activation and disease pathogenesis remain unclear. Future studies are essential to elucidate these mechanisms and their broader consequences in the immunopathogenesis of viral infections.

Our study has several significant implications, we explored the pathogenic role of serum IgA antibodies, a frequently overlooked antibody isotype in immune responses. Our findings highlight the critical interplay between antigenic target and antibody isotype in disease and protection. While IgA antibodies targeting E can counteract ADE from IgG against the structural components of the virion[30] and IgG anti-NS1 antibodies confer protection against the virulent properties of NS1[43,44], our results show that anti-NS1 IgA antibodies are implicated in severe disease. Furthermore, while we do not exclude IgG-mediated ADE, our observations support the presence of an alternative pathogenic pathway mediated by IgA antibodies and neutrophil activation in DENV infection. This highlights an interesting therapeutic avenue, since neutrophil functions can be targeted by approved and emerging drugs[45]. Moreover, our findings underscore the importance of evaluating isotype- and antigen-specific antibody profiling of humoral immune responses induced by DENV and ZIKV vaccines. While further validation across diverse geographic and demographic settings is needed, our results suggest that IgA binding and avidity may serve as predictive markers of subsequent severe dengue disease. Similarly, the assessment

of neutrophil degranulation early during DENV infection could provide a valuable triaging tool for identifying patients at risk of DHF/DSS.

Finally, our findings enrich the current understanding of the role of pre-existing immunity in the immunopathogenesis of severe dengue disease. Using binding assays, *ex-vivo* functional assays, and validation of our observations in paired pre-infection and acute samples as well as an orthogonal study, we show that IgA antibodies drive neutrophil activation that correlates with increased risk of severe disease and precedes vascular leakage. We underscore the importance of antibody isotypes beyond IgG, such as IgA, and their antigenic targets (NS1 vs. E), with implications for establishing biomarkers of risk, refining therapeutic strategies and informing vaccine development. Further research into the precise mechanisms of IgA-mediated neutrophil activation is essential to fully unravel the pathways driving severe disease in the context of flaviviral and other infectious diseases.

Materials and Methods

Ethics statement

The Pediatric Dengue Cohort Study was reviewed and approved by the institutional review boards of the University of California, Berkeley (protocol 2010-09-2245), the University of Michigan (HUM00091606), and the Nicaraguan Ministry of Health (NIC-MINSA/CNDR CIRE-09/03/07-008). The Pediatric Dengue Hospital-based Study was reviewed and approved by the institutional review boards of the University of California, Berkeley (2010-06-1649) and the Nicaraguan Ministry of Health (NIC-MINSA/CNDR CIRE-01/10/06-13). Parents or legal guardians of all subjects provide written informed consent, and subjects ≥6 years old provide assent.

Study design

The primary objective of this study was to identify antibody biomarkers associated with the risk of developing severe dengue after a primary ZIKV infection during a subsequent DENV2 infection. Serum samples were obtained from participants enrolled in the Pediatric Dengue Cohort Study (PDCS), as described below. These participants had a documented primary ZIKV infection

in 2016 and then experienced a DENV2 infection in the 2019-2020 dengue season. During the DENV2 infection, children developed either dengue fever (DF, n=14) or dengue hemorrhagic fever/dengue shock syndrome (DHF/DSS, n=10). We evaluated serum samples collected after the primary ZIKV infection and 4-10 months before the secondary DENV2 infection in order to identify antibody biomarkers of risk, using our multiplexed bead-based approach[12], as described below.

The primary endpoint was the clinical classification of DF versus DHF/DSS, based on the WHO 1997 guidelines (see below). Secondary endpoints included the presence of plasma leakage, hemorrhagic manifestations, and thrombocytopenia. We also used gallbladder wall thickness, assessed by ultrasonography, as a surrogate of vascular leak[23].

Following the identification of humoral biomarkers correlated with clinical outcomes (i.e., IgA antibodies targeting the viral NS1 protein), we investigated their role in disease pathogenesis. Given that neutrophils are the most abundant and primary effectors of IgA antibodies[16], we performed *ex vivo* functional assays to evaluate antibody-dependent neutrophil effector functions (see below). Additionally, we examined the involvement of neutrophils and their correlation with antibody binding using paired acute-phase samples from the same participants of the PDCS during the acute secondary DENV2 infection. Finally, the findings were further validated with an independent dataset from the Pediatric Dengue Hospital Study (PDHS), evaluating participants who experienced a DENV2 infection during 2018 to 2020 with a history of primary ZIKV infection.

Description of studies

The **Pediatric Dengue Cohort Study (PDCS)** is an ongoing prospective cohort study initiated in 2004 and based at the Sócrates Flores Vivas Health Center (HCSFV), the primary health care facility for District II of Managua, and part of the Municipal Health System of Managua. Located adjacent to Lake Xoxitlan, District 2 encompasses neighborhoods spanning a spectrum of low to middle socioeconomic status. The HCSFV serves ~62,000 residents across 18 neighborhoods within District II[46]. The illiteracy rate in this area is approximately 7%, and over 90% of the households have access to running water and a sewage system. All residents have access to electricity. The PDCS tracks approximately 4,000 active participants yearly and has

followed ~9,800 children since its initiation. To preserve the original age distribution of the cohort, approximately 250 two-year-old children, along with children aged 3-11 years as needed, are enrolled annually. Adjustments to the age limit were implemented in 2018, 2019, and 2022, extending the eligibility to 15, 16, and 17 years, respectively. Participants benefit from free, round-the-clock medical care provided by study physicians at the HCSFV. In cases requiring hospitalization, study staff facilitate patient transfer to the study hospital, the National Pediatric Reference Hospital (Hospital Infantil Manuel de Jesús Rivera). Children presenting with fever and, since July 2016, rash are screened for signs and symptoms of dengue, Zika, and chikungunya. Symptomatic infections are captured through "enhanced" passive surveillance, complemented with periodic home visits. For each suspected case, both acute (0-6 days post-symptom onset) and convalescent samples (14-21 days) are collected to confirm infection. Approximately 97% of cases present to the HCSFV within the first three days of illness, and convalescent samples are collected from 94% of cases (Kuan et al 2009 AJE). Additionally, the study collects annual healthy blood samples from all participants in March-April (previously in July before 2011), which enables the detection of inapparent arboviral infections[10].

The **Pediatric Dengue Hospital-Based Study (PDHS)** is based at the Hospital Infantil Manuel de Jesús Rivera (HIMJR), Managua, Nicaragua (2005-present)[22,47]. Children are invited to participate if they: 1) present to the hospital 1-7 days post-onset of symptoms and 2) meet case definitions for dengue, Zika, and/or chikungunya, which consists of either i) ≥1 signs or symptoms, including headache, arthralgia, myalgia, retro-orbital pain, positive tourniquet test, petechiae, or signs of bleeding; or ii) rash with ≥2 signs/symptoms including fever, conjunctivitis, arthralgia, myalgia, or peri-articular edema[22]. Blood samples are collected at presentation (acute), daily for days 1-3, and at convalescence (14-28 days). Infections are defined as for the cohort using RT-PCR, virus isolation, and DENV, ZIKV, and CHIKV serological assays (detailed below). Clinical information (>150 variables) and fluid intake/output is collected every 12 hours, and, after systematic monitoring by a clinical supervisor, is digitized by double-data entry, with quality control checks performed daily and weekly. A standardized questionnaire is used to record the subject's demographic and epidemiologic characteristics. As part of a longitudinal arm of the study, consenting participants return to provide healthy blood samples 3, 6, 12, and 18 months post-illness.

Case definitions

Primary ZIKV infection in the PDCS was defined as DENV- and ZIKV-naïve participants who presented with fever or rash after July 2016 and were clinically classified as either: A) meeting the 1997 and/or 2009 WHO criteria for dengue, or B) having an undifferentiated febrile illness. Laboratory confirmation of ZIKV infection was performed as described below.

Primary ZIKV infection in the PDHS was defined as participants meeting criteria A or B during 2018–2019 and showing evidence of a monotypic ZIKV antibody response early in infection (<4 days post-fever onset), as defined in [4] or [12] (detailed below).

Second DENV2 infection was defined as children who met the criteria for primary ZIKV infection and subsequently developed a DENV2 infection during 2019–2020 in the PDCS or 2018–2020 in the PDHS. Children experiencing a second DENV2 infections were classified as DF or DHF/DSS based on the criteria described below.

Laboratory confirmation of ZIKV and DENV infections in the PDCS

All cases meeting definitions A or B were evaluated for acute ZIKV or DENV infections, with laboratory confirmation performed by: 1) real-time RT-PCR (rRT-PCR) and/or viral isolation from acute serum (and/or urine for ZIKV); 2) seroconversion detected via ZIKV or DENV IgM capture (MAC)-ELISA; and/or 3) seroconversion or a ≥4-fold increase in DENV- or ZIKV-specific iELISA titers in paired acute and convalescent sera[10,48]. The infecting virus (DENV or ZIKV) was determined based on rRT-PCR results[49,50]. RT-PCR-negative cases were classified as 1) ZIKV if seroconversion or a ≥4-fold rise in ZIKV-specific titers was detected, or, for arbovirus cases in 2016–2017, if identified as ZIKV-positive by a computational classification algorithm[51], or 2) Flavivirus cases if seroconversion or a ≥4-fold increase was observed in both DENV and ZIKV assays. Flavivirus cases and cases with confirmed RT-PCR or viral isolation evidence of co-infection with DENV and ZIKV were excluded from the analyses. All secondary DENV2 infections were confirmed by rRT-PCR[49].

Inclusion and exclusion criteria

All participants from the PDCS who had a documented primary ZIKV infection in 2016 followed by a second DENV2 infection during 2019-2020, with the second infection classified as DHF/DSS according to WHO 1997 criteria, were included (n=10). Additionally, 14 participants with a similar infection history who developed DF, matched by sex and age, were selected as a comparison group using convenience sampling. The entire sample set was used for analysis of neutrophil counts during infection, excluding 7 participants with missing neutrophil counts on day 3 post-fever onset (Fig. 3B).

In the PDHS, a total of 362 confirmed DENV2 infections were documented between 2018 and 2020. Among these, 261 cases were classified as DF and 65 as DHF/DSS. All 65 DHF/DSS and a convenience sample of 103 DF cases were serotyped to identify second DENV2 infections after a primary ZIKV, using the methods described in [4] and [12] (detailed below). A total of 111 participants with past ZIKV infections were identified (DF=67, DHF/DSS=44). This entire sample set was used for analysis of neutrophil counts during infection, excluding 2 participants with missing neutrophil counts (Fig. 4A).

For our orthogonal confirmation of neutrophil involvement during acute DENV2 infection, we determined the sample size using Cohen's *d* effect size and power analysis[52]. Based on our observations in the PDCS, the estimated effect size was $d = -0.9128$ (95% CI: -1.8139, -0.0117), corresponding to a large effect size. To achieve a statistical power of 80% ($\beta = 0.20$) at a significance level of 0.05 ($\alpha = 0.05$) for a one-tailed two-sample *t*-test (assuming normal data distribution), a minimum of 16 participants per group (DF vs. DHF/DSS) was required. Accordingly, to analyze the temporal relationship between neutrophil functions and progression to severe disease, we selected a subsample of 18 DHF/DSS cases with serum samples collected on day 3 post-fever onset or earlier. These cases were matched by sex and age with 36 DF cases whose serum samples were also collected during acute infection (day 3 post-fever onset or earlier). This dataset was used to compare neutrophil degranulation among clinical groups and to evaluate the correlation of neutrophil degranulation with the maximum documented thickness of the gallbladder wall. Participant characteristics are summarized in **Table S1**. The plot in Fig. 4C included 7 DF and 10 DHF/DSS with gallbladder thickness information from the PDCS, and 66 participants with DF and 43 participants with DHF/DSS from the PDHS.

Definition of severe dengue disease

Severe disease in our study was defined as a composite outcome of children meeting the WHO 1997 criteria for Dengue Hemorrhagic Fever or Dengue Shock Syndrome. **Dengue Hemorrhagic Fever** was defined as experiencing at least one of each of the following criteria: fever plus 1) hemorrhagic manifestations defined as the presence of at least one of the following manifestations: i) positive tourniquet test, ii) ecchymosis, petechia, hematoma, purpura, iii) bleeding at injection site, hypermenorrhea or vaginal bleeding, subconjunctival hemorrhage, hematuria, hemoptysis, bleeding gums or nose, iv) hematemesis or melena; 2) thrombocytopenia defined as platelet count $\leq$100,000 platelets per mm^3; 3) evidence of plasma leakage as a result of increased vascular permeability defined as i) $\geq$20% hemoconcentration, ii) age- and sex-specific elevated hematocrit, iii) pleural effusion, iv) ascites, v) hypoproteinemia or hypoalbuminemia, or vi) edema. **Dengue Shock Syndrome** (1997 WHO criteria) was defined as cases meeting criteria for DHF and at least one of each of the following criteria: 1) i) age-specific hypotension or ii) narrow pulse pressure <20 mmHg), and 2) i) cold, clammy skin and restlessness or ii) rapid and weak pulse. Symptomatic participants infected with DENV2 who did not meet the criteria for severe disease were categorized as having **Dengue Fever (DF)**. Additionally, secondary endpoints for the study included the presence of hemorrhagic manifestations, thrombocytopenia, or plasma leakage, as defined by the established criteria.

Viral load quantification

Viral RNA was extracted from virus particles using the QIAmp kit (QIAGEN). The PCR standard curve used for the quantification of DENV genome copies was obtained with an amplicon containing a synthetic cDNA encompassing a fragment of the NS5 region (nucleotides 9937–10113) from DENV2 strain DENV2 (8971.12a1SPD2; Genbank; MZ008454.1). Absolute quantitation of viral RNA was determined by real-time quantitative RT-PCR (RT-qPCR) using the following primer and probe sequences: DENV2 forward (ACAAGTCGAACAACCTGGTCCAT), reverse (GCCGCACCATTGGTCTTCTC) and probe (FAM- CCAGTGGAATCATGGGAAGAAGTCC CA-TAMRA. The Verso 1-step RT-qPCR kit (Thermo Fisher Scientific) was used following the manufacturer's instructions. Standard curves were prepared using seven 10-fold dilutions of a DENV2 (8971.12a1SPD2; Genbank;

MZ008454.1) synthetic fragment. Reaction mixtures were run in a QuantStudio 3 thermocycler (Applied Biosystems), and the quantity values were used for analyses[53,54].

EDIII serotyping in the PDHS

The EDIII serotyping of early acute serum samples (<4 days post-fever onset) from the PDHS was conducted as described in[12]. Briefly, recombinant EDIII proteins for DENV1-4 and ZIKV (courtesy of Dr. Lakshmanane Premkumar, University of North Carolina [UNC], Chapel Hill) were site-specifically biotinylated and conjugated to avidin-coated MagPlex Luminex beads. These antigen-coupled microspheres were combined and incubated in 384-well plates with appropriately diluted plasma (four 4-fold dilutions starting at 1:50). Each well contained 500 microspheres per antigen and was incubated for 90 minutes at 37°C, shaking at 1200 rpm. Following incubation, the plates were washed with phosphate-buffered saline (PBS) containing 0.1% bovine serum albumin (BSA) and 0.02% Tween 20 using an automatic magnetic washer (Tecan Hydrospeed). Antigen-specific IgG binding was detected with phycoerythrin (PE)-conjugated mouse anti-human total IgG (SouthernBiotech #9040-09). Median fluorescence intensity (MFI) was measured using an iQue3 (Intellicyt) instrument, set to acquire at least 50 beads per bead region. DENV-naïve human serum was included in triplicate on each plate as a negative control. MFI values for EDIII-DENV1, EDIII-DENV2, EDIII-DENV3, EDIII-DENV4, and EDIII-ZIKV were transformed as the relative proportion of the highest MFI observed at a serum dilution of 1:800. Then, a heatmap with hierarchical clustering using Wald's method was generated, identifying five distinct clusters corresponding to DENV1-4 and ZIKV. The prior infecting virus (DENV1-4 or ZIKV) was assigned based on the antigen with the highest MFI value and the grouping within the cluster analysis. Finally, an empirical cutoff value was applied to distinguish monotypic EDIII ZIKV responses[12]. Specifically, for a sample to be classified as past primary ZIKV infection, the second highest MFI signal should be lower than 20% of the maximum ZIKV EDIII signal. Prior ZIKV infections were successfully detected in acute-phase sera from the PDHS using a similar EDIII-based method in[4].

Multiplex bead-based antibody binding and avidity assay

Recombinant E and NS1 proteins from DENV1-4 and ZIKV were commercially acquired from Native Antigen Co. (United Kingdom). Recombinant EDIII of DENV1-4 and ZIKV were

site-specifically biotinylated and provided as a gift by Dr. Premkumar (UNC, Chapel Hill). Antibody subclass and isotype binding in pre-infection samples was determined using a multiplex bead-based assay, as previously described[12]. Briefly, E and NS1 from DENV1-4 and ZIKV were randomly biotinylated according to the manufacturer's instructions (EZ-Link™ Sulfo-NHS-LC-LC-Biotin, No-Weigh™ Format; Thermo Fisher Scientific) and desalted using Zeba Spin Columns (Thermo Fisher Scientific). The randomly biotinylated E and NS1 and the site-specifically biotinylated EDIII from DENV1-4 and ZIKV were conjugated to avidin-coated MagPlex Luminex beads. Immune complexes were formed in 384-well plates by mixing the appropriately diluted plasma (six 4-fold dilutions) with antigen-coupled microspheres for 90 minutes at 37°C, shaking at 1200 rpm. After incubation, plates were washed using an automatic magnetic washer (Tecan Hydrospeed) with PBS containing 0.1% BSA and 0.02% Tween 20. For avidity testing, samples were washed for ten minutes with urea 7M or with PBS. Afterward, plates were washed again with PBS containing 0.1% BSA and 0.02% Tween 20. Finally, antigen-specific subclass/isotype binding was detected using PE-coupled mouse anti-human detection antibodies against IgA (SouthernBiotech #2050-09), IgM (SouthernBiotech #9020-09), total IgG (SouthernBiotech #9040-09), IgG1 (Southern-Biotech #9052-09), IgG2 (SouthernBiotech #9060-09), IgG3 (Southern-Biotech #9210-09), and IgG4 (SouthernBiotech #9200-09). Fluorescence was acquired using an iQue3 (Intellicyt) machine (Sartorius), as described above. Antigen-specific antibody subclass/isotype binding was extracted as median fluorescence intensity (MFI). Then, a netMFI was calculated by subtracting the background binding of a DENV-naïve sample from each test sample. Then, we fitted a dose-response curve using the netMFI across six 4-fold serial dilutions of plasma to estimate the effective dilution 50 (ED_{50}) of the binding for each tested antigen, antibody subclass/isotype, and participant using the *drda* package v2.0.3. For calculating the Avidity Index (AI), the area under the curve (AUC) of the binding after washing with Urea or PBS was estimated, and then compared using the formula AI = AUC[Urea]/AUC[PBS]. Antigen-specific binding in acute phase samples was performed with E, NS1, and E dimer from DENV2. The recombinant stabilized envelope E dimer of DENV2 was purchased from the UNC Protein Expression and Purification Core[55]. Binding during the acute phase was analyzed as the AUC of the binding curve fitted using a dose-response model[54].

<u>IgA depletion from serum</u>

IgA antibodies were depleted from serum using the CaptureSelect™ IgA-XL Affinity Matrix resin (Thermo Scientific™) with a spin column method. Briefly, disposable Mobicol spin columns were prepared by loading either the CaptureSelect™ IgA affinity resin for depletion or empty agarose beads for mock depletion. The resins were equilibrated with PBS (pH 7.4) prior to sample application to ensure optimal binding conditions.

For depletion or mock-depletion, human serum diluted 1:50 was applied to the column containing the IgA-specific resin or empty resin. The column was incubated on a rotating wheel at room temperature for 30 minutes to allow antibody binding. After incubation, the column was centrifuged at 700 × g for 1 minute to collect the flow-through, which contained the IgA-depleted or mock depleted serum. Antibody binding, IgA depletion, and mock-depletion was confirmed in validation samples using the previously described antibody binding and isotype characterization multiplex bead-based protocol. Depleted and mock-depleted samples were stored at -80°C until further analysis.

Antibody-dependent neutrophil phagocytosis and NETosis

Functional neutrophil *ex vivo* assays were conducted using neutrophils from three independent healthy human donors: two donors for antibody-dependent neutrophil phagocytosis (ADNP) and one donor for NETosis. Neutrophils were stimulated with immune complexes formed from pre-infection serum antibodies and the antigen of interest, as detailed below.

ADNP was performed as previously described[20]. Antigens (NS1-DENV2 or E-DENV2, Native Antigen Co.) were biotinylated and coupled to yellow-green neutravidin beads (Invitrogen). Immune complexes were formed by mixing coupled beads and appropriately diluted plasma and incubating for 2 hours at 37°C. White blood cells were isolated from fresh peripheral blood from healthy donors by performing ammonium-chloride-potassium lysis of red blood cells. The isolated white blood cells were then added to 96-well plates at a concentration of 2.5×10^5 cells/ml, and neutrophils were identified using anti-CD66b PacBlue (BioLegend, 305112). Fluorescence was acquired using an iQue3 machine. A phagocytic score was calculated using the following formula: (percentage of bead-positive cells) x (geometric mean of MFI of bead-positive cells)/10,000. The results were summarized as the mean of the two independent experiments for each serum sample, and the value was normalized using the min-max approach.

For NETosis, neutrophils were isolated from whole blood collected in EDTA tubes from one healthy donor under protocol #2303138796A001 at the Ponce Health Sciences University and Ponce Research Institute in Puerto Rico, using the EasySep Direct Human Neutrophil Isolation Kit (Stemcell Technologies, Catalog #19666). Cells were resuspended in Gibco Opti-MEM Serum Reduced Media (ThermoFisher, Catalog #31985070). To generate fixed immune complexes (ICs), NS1 or E protein (2 μg/mL) was plated in a 96-well plate and incubated overnight at 4°C with medium (negative control), Phorbol myristate acetate (PMA) as positive control, and mock-depleted or IgA-depleted samples. After protein coating, wells were washed three times with 1X PBS and then incubated with a 1:25 dilution of serum in 1X PBS (100 μL per well) overnight at 4°C. Wells were then washed three times with sterile 1X PBS containing 0.05% Tween 20 and then one time with 1X PBS before adding neutrophils. Neutrophils (30,000 cells/well) were added to each well in 100 μL of Gibco Opti-MEM containing 250 nM Cytotox Green (Essen BioScience, Catalog #4633). Plates were placed in an Incucyte SX5 instrument (Sartorius AG, Göttingen, Germany) for live-cell imaging. Phase-contrast and green fluorescence images were captured at 20X magnification, with an exposure time of 300 milliseconds for green fluorescence. Images were acquired every 30 minutes for 6 hours, with two images per well from distinct regions. The Incucyte software was trained to differentiate between normal cells and those undergoing DNA release using representative images from non-stimulated and stimulated cells. For analysis, the software applied surface-fit background correction with a fluorescence threshold of 2.0 Green Calibrated Units (GCU), edge sensitivity of -25, and a minimum mean intensity of 100. Phase-contrast analysis used artificial intelligence (AI) confluence detection. The software automatically analyzed the images and calculated the total integrated green intensity (GCU x μm^2/ image) per well to quantify DNA release associated with NETosis. Paired IgA-depleted and mock-depleted samples were compared for each antigen to calculate the percentage of signal loss due to IgA depletion. To ensure comparability across samples, the percentage of signal loss was determined at the timepoint of the slope of the positive control (after one hour of stimuli) using the formula: Percentage change in signal = (IgA-depleted - IgA mock-depleted)/IgA mock-depleted * 100. The results were expressed as percentages, ranging from -100% to +100%.

<u>Quantification of markers of neutrophil degranulation</u>

Neutrophil degranulation and NETosis were assessed in serum immediately after thawing, using commercially available kits following the manufacturers' protocols.

Myeloperoxidase (MPO) and Matrix Metalloproteinase-9 (MMP9) concentrations in plasma were quantified using DuoSet™ ELISA kits (R&D Systems, DY3174 and DY911, respectively). Briefly, 96-well plates were coated with specific capture antibodies diluted in PBS (pH 7.2–7.4) and incubated overnight at room temperature. Plates were blocked with 1% BSA in PBS for 1 hour at room temperature. Samples and standards, diluted in PBS with 1% BSA (with 2% normal goat serum for MMP9), were added (100 µL/well) and incubated for 2 hours at room temperature. Detection antibodies conjugated to biotin were applied, followed by a 20-minute incubation with streptavidin-horse radish peroxidase (HRP). Signal development was achieved using tetramethylbenzidine (TMB), and the reaction was stopped with 2N sulfuric acid. Optical density (OD) was measured at 450 nm with background correction at 570 nm. Standard curves were generated using serial dilutions of recombinant MPO and MMP9, and sample concentrations were interpolated using linear regression.

Human neutrophil elastase (NE) concentrations in plasma were quantified using the Hycult Biotech commercial kit (HK319). Plasma samples were diluted and added to microtiter wells pre-coated with a human elastase-specific capture antibody. Standards and samples (100 µL/well) were incubated for 1 hour at room temperature. After washing four times with wash buffer, 100 µL of biotinylated tracer antibody was added, and the plate was incubated for another hour at room temperature. Following additional washes, 100 µL of streptavidin-peroxidase conjugate was applied, and the plate was incubated for 1 hour. Signal development was performed by adding 100 µL of TMB substrate and incubating for 30 minutes in the dark. The reaction was terminated with 2% oxalic acid, and absorbance was measured at 450 nm using a microplate reader.

Human lactoferrin levels in plasma were measured using the CatchPoint® SimpleStep ELISA® kit (ab229392, Abcam), which employs fluorescence detection. Plasma samples were processed following the manufacturer's recommendations. Standards were prepared by serial dilutions from a reconstituted lactoferrin stock solution. Standards and samples (50 µL each) were added to pre-coated wells, followed by 50 µL of an antibody cocktail containing capture and detector antibodies. Plates were incubated for 1 hour at room temperature on a plate shaker set to

400 rpm and subsequently washed three times with Wash Buffer. Detection was performed by adding 100 µL of CatchPoint HRP Development Solution, containing Stoplight Red Substrate and hydrogen peroxide, followed by a 10-minute incubation in the dark. Fluorescence intensity was measured at 530 nm (excitation), 570 nm (cutoff), and 590 nm (emission) using a fluorescence plate reader.

Neutrophil extracellular traps (NETs) in plasma samples were quantified using the GENLISA™ Human NETs ELISA Kit (KBH4548, Krishgen BioSystems). Plasma samples were diluted in the Standard Diluent provided. A standard curve was generated using serial dilutions of the NETs standard stock solution. Samples and standards (100 µL each) were added to wells of a microtiter plate pre-coated with anti-NETs antibodies, followed by a 60-minute incubation at 37°C. After aspiration, 100 µL of Biotinylated NETs Antibody Working Solution was added, and the plate was incubated for another 60 minutes at 37°C. Wells were then washed four times with 1X Wash Buffer to remove unbound components. Next, 100 µL of Streptavidin-HRP Working Solution was added to each well and incubated for 30 minutes at 37°C. Following additional washes, 100 µL of TMB substrate was added to develop the signal during a 10-minute incubation in the dark at 37°C. The reaction was terminated by adding 100 µL of Stop Solution. Absorbance was measured at 450 nm using a microplate reader within 15 minutes of adding the Stop Solution.

A standard curve was generated by plotting absorbance or fluorescence values against known analyte concentrations, and sample concentrations were interpolated and adjusted for dilution factors. Background correction was performed by subtracting the blank (zero standard) signal from all optical density (OD) or fluorescence values. Samples exceeding the upper limit of quantification were reanalyzed at higher serum dilutions when possible; otherwise, data was analyzed as background-corrected OD or fluorescence values. All assays were conducted in duplicate, and results were reported as the mean of the technical replicates. Outliers were identified and removed using the Interquartile Range (IQR) method. Boundaries for identifying outliers were defined as follows: Lower Bound: Q1 – (1.5 × IQR); Upper Bound: Q3 + (1.5 × IQR). Observations with values outside these thresholds were considered outliers and excluded from further analysis.

Statistical analysis

All statistical analyses were performed using R (v4.2.3, R Foundation for Statistical Computing). Differences in the ED_{50} of binding antibodies in pre-infection samples between children who subsequently experienced DF or DHF/DSS were analyzed using a two-tailed Wilcoxon rank-sum test with false discovery rate (FDR) correction for multiple comparisons. Logistic regression models were employed to evaluate the association between pre-existing antibody profiles and the subsequent development of DHF/DSS. Each antibody characteristic was analyzed in a separate regression model, with FDR correction applied for multiple hypothesis testing.

To adjust the coefficients of the antibody characteristics correlated with DHF/DSS, we performed a multivariate regression with regularization. To estimate the regularization parameters, the dataset was divided into training and testing sets (50-50 split). Optimal regularization parameters (gamma and alpha) were determined via bootstrapping (n=1000), maximizing the area under the curve (AUC) on the training set. Then, the optimal parameters were applied to re-estimate the coefficients for selected antibody features using the entire dataset. Regularization was implemented using the glmnet R package (v4.1-860).

To compare the predictive accuracy of Total IgA versus Total IgG antibody avidity in pre-infection samples for distinguishing the children who subsequently developed DF or DHF/DSS, a similar regularization approach was used. In addition, the variables in the final model were assessed using an orthogonal partial least squares discriminant analysis (OPLS-DA) to estimate the variance in the response variable explained by the model (R^2Y), the predictive performance for new data (Q^2), and the overall classification accuracy. Three models were compared: avidity of IgA antibodies alone, avidity of IgG antibodies alone, and a model including avidity of IgA + IgG.

Normalized phagocytic scores, percentage changes in signal in the NETosis assay, relative neutrophil counts, and levels of degranulation markers were compared across clinical groups using a one-tailed Wilcoxon rank-sum test. Logistic regression was employed to assess the association between degranulation marker levels and severe disease manifestations, estimating odds ratios (ORs) and 95% confidence intervals (CIs) using the oddsratio package (v2.0.1). Linear regression was used to evaluate the relationships between degranulation markers and antibody binding

profiles, as well as between degranulation markers and maximum gallbladder wall thickness. All statistical analyses were conducted at a significance level of 5%.

References

1. Bhatt, S. *et al.* The global distribution and burden of dengue. *Nature* **496**, 504–507 (2013).
2. Paz-Bailey, G., Adams, L. E., Deen, J., Anderson, K. B. & Katzelnick, L. C. Dengue. *The Lancet* **403**, 667–682 (2024).
3. Katzelnick, L. C. *et al.* Antibody-dependent enhancement of severe dengue disease in humans. *Science (1979)* **358**, 929–932 (2017).
4. Katzelnick, L. C. *et al.* Zika virus infection enhances future risk of severe dengue disease. *Science (1979)* **369**, 1123–1128 (2020).
5. Zambrana, J. V. *et al.* Primary exposure to Zika virus is linked with increased risk of symptomatic dengue virus infection with serotypes 2, 3, and 4, but not 1. *Sci Transl Med* **16**, 2199 (2024).
6. Yamanaka, A. *et al.* Antibody-dependent enhancement representing in vitro infective progeny virus titer correlates with the viremia level in dengue patients. *Sci Rep* **11**, (2021).
7. Waggoner, J. J. *et al.* Antibody-Dependent Enhancement of Severe Disease Is Mediated by Serum Viral Load in Pediatric Dengue Virus Infections. *J Infect Dis* **221**, 1846–1854 (2020).
8. Bournazos, S. *et al.* Antibody fucosylation predicts disease severity in secondary dengue infection. *Science (1979)* **372**, 1102–1105 (2021).
9. Yamin, R. *et al.* Human FcγRIIIa activation on splenic macrophages drives dengue pathogenesis in mice. *Nat Microbiol* **8**, 1468–1479 (2023).
10. Gordon, A. *et al.* The Nicaraguan Pediatric Dengue Cohort Study: Incidence of Inapparent and Symptomatic Dengue Virus Infections, 2004–2010. *PLoS Negl Trop Dis* **7**, e2462 (2013).
11. Estofolete, C. F. *et al.* Influence of previous Zika virus infection on acute dengue episode. *PLoS Negl Trop Dis* **17**, e0011710 (2023).
12. Bos, S. *et al.* Serotype-specific epidemiological patterns of inapparent versus symptomatic primary dengue virus infections: a 17-year cohort study in Nicaragua. *Lancet Infect Dis* (2024) doi:10.1016/S1473-3099(24)00566-8.
13. Perciani, C. T., Peixoto, P. S., Dias, W. O., Kubrusly, F. S. & Tanizaki, M. M. Improved method to calculate the antibody avidity index. *J Clin Lab Anal* **21**, 201–206 (2007).

14. Shackelford, P. G., Granoff, D. M., Madassery, J. V, Scott, M. G. & Nahm, M. H. Clinical and Immunologic Characteristics of Healthy Children with Subnormal Serum Concentrations of IgG2. *Pediatr Res* **27**, 16–21 (1990).
15. Plebani, A. *et al.* Serum IgG subclass concentrations in healthy subjects at different age: Age normal percentile charts. *Eur J Pediatr* **149**, 164–167 (1989).
16. Steffen, U. *et al.* IgA subclasses have different effector functions associated with distinct glycosylation profiles. *Nat Commun* **11**, 120 (2020).
17. Mayer-Hain, S. *et al.* Systemic Activation of Neutrophils by Immune Complexes Is Critical to IgA Vasculitis. *J Immun* **209**, 1048–1058 (2022).
18. Pillebout, E. IgA Vasculitis and IgA Nephropathy: Same Disease? *J Clin Med* **10**, 2310 (2021).
19. Aroca-Crevillén, A., Vicanolo, T., Ovadia, S. & Hidalgo, A. Neutrophils in Physiology and Pathology. *Annu Rev Pathol* **19**, 227–259 (2024).
20. Dias, A. G. *et al.* Antibody Fc characteristics and effector functions correlate with protection from symptomatic dengue virus type 3 infection. *Sci Transl Med* **14**, 3151 (2022).
21. Strich, J. R. *et al.* Fostamatinib Inhibits Neutrophils Extracellular Traps Induced by COVID-19 Patient Plasma: A Potential Therapeutic. *J Infect Dis* **223**, 981–984 (2021).
22. Narvaez, F. *et al.* Dengue severity by serotype and immune status in 19 years of pediatric clinical studies in Nicaragua. *PLoS Negl Trop Dis* **19**, e0012811 (2025).
23. Colbert, J. A. *et al.* Ultrasound measurement of gallbladder wall thickening as a diagnostic test and prognostic indicator for severe dengue in pediatric patients. *Pediatr Infect Dis J* **26**, 850–852 (2007).
24. Ferreira, B. D. C. & Correia, D. Ultrasound Assessment of Hepatobiliary and Splenic Changes in Patients With Dengue and Warning Signs During the Acute and Recovery Phases. *J Ultrasound Med* **38**, 2015–2024 (2019).
25. Srikiatkhachorn, A. *et al.* Natural History of Plasma Leakage in Dengue Hemorrhagic Fever. *Pediatr Infect Dis J* **26**, 283–290 (2007).
26. Ruchusatsawat, K. *et al.* Long-term circulation of Zika virus in Thailand: an observational study. *Lancet Infect Dis* **19**, 439–446 (2019).
27. Monteiro, R. C. & Suzuki, Y. Are there animal models of IgA nephropathy? *Semin Immunopathol* **43**, 639–648 (2021).

28. Seminario, G. *et al.* The Latin American Society for Immunodeficiencies Registry. *J Clin Immunol* **45**, 28 (2024).
29. Wang, Z. *et al.* Enhanced SARS-CoV-2 neutralization by dimeric IgA. *Sci Transl Med* **13**, 1555 (2021).
30. Wegman, A. D. *et al.* DENV-specific IgA contributes protective and non-pathologic function during antibody-dependent enhancement of DENV infection. *PLoS Pathog* **19**, e1011616 (2023).
31. Upadhaya, B. K. *et al.* Transient IgA nephropathy with acute kidney injury in a patient with dengue fever. *Saudi J Kidney Dis Transpl* **21**, 521–5 (2010).
32. Bachal, R. *et al.* Higher levels of dengue-virus-specific IgG and IgA during pre-defervescence associated with primary dengue hemorrhagic fever. *Arch Virol* **160**, 2435–2443 (2015).
33. Chia, P. Y., Teo, A. & Yeo, T. W. Association of Neutrophil Mediators with Dengue Disease Severity and Cardiac Impairment in Adults. *J Infect Dis* **226**, 1974–1984 (2022).
34. Loke, P. *et al.* Gene Expression Patterns of Dengue Virus-Infected Children from Nicaragua Reveal a Distinct Signature of Increased Metabolism. *PLoS Negl Trop Dis* **4**, e710 (2010).
35. Recker, M. *et al.* Markers of prolonged hospitalisation in severe dengue. *PLoS Negl Trop Dis* **18**, e0011922 (2024).
36. Robinson, M. *et al.* A 20-Gene Set Predictive of Progression to Severe Dengue. *Cell Rep* **26**, 1104-1111.e4 (2019).
37. Liu, Y. E. *et al.* An 8-gene machine learning model improves clinical prediction of severe dengue progression. *Genome Med* **14**, 33 (2022).
38. Duggal, S. *et al.* Dengue virus infection in mice induces bone marrow myeloid cell differentiation and generates Ly6Glow immature neutrophils with modulated functions. *J Leukoc Biol* **115**, 130–148 (2024).
39. Stacey, H. D. *et al.* IgA potentiates NETosis in response to viral infection. *Proc Natl Acad Sci U S A* **118**, (2021).
40. Gimpel, A.-K. *et al.* IgA Complexes Induce Neutrophil Extracellular Trap Formation More Potently Than IgG Complexes. *Front Immunol* **12**, 761816 (2021).
41. Knackstedt, S. L. *et al.* Neutrophil extracellular traps drive inflammatory pathogenesis in malaria. *Sci Immunol* **4**, 336 (2019).

42. Passelli, K. *et al.* The c-MET receptor tyrosine kinase contributes to neutrophil-driven pathology in cutaneous leishmaniasis. *PLoS Pathog* **18**, e1010247 (2022).
43. Biering, S. B. *et al.* Structural basis for antibody inhibition of flavivirus NS1–triggered endothelial dysfunction. *Science (1979)* **371**, 194–200 (2021).
44. Modhiran, N. *et al.* A broadly protective antibody that targets the flavivirus NS1 protein. *Science (1979)* **371**, 190–194 (2021).
45. Németh, T., Sperandio, M. & Mócsai, A. Neutrophils as emerging therapeutic targets. *Nat Rev Drug Discov* **19**, 253–275 (2020).
46. Gordon, A. *et al.* The Nicaraguan pediatric influenza cohort study: design, methods, use of technology, and compliance. *BMC Infect Dis* **15**, 504 (2015).
47. Narvaez, F. *et al.* Evaluation of the Traditional and Revised WHO Classifications of Dengue Disease Severity. *PLoS Negl Trop Dis* **5**, e1397 (2011).
48. Balmaseda, A. *et al.* Comparison of Four Serological Methods and Two Reverse Transcription-PCR Assays for Diagnosis and Surveillance of Zika Virus Infection. *J Clin Microbiol* **56**, e01785-17 (2018).
49. Waggoner, J. J. *et al.* Single-Reaction, Multiplex, Real-Time RT-PCR for the Detection, Quantitation, and Serotyping of Dengue Viruses. *PLoS Negl Trop Dis* **7**, e2116 (2013).
50. Waggoner, J. J. *et al.* Single-Reaction Multiplex Reverse Transcription PCR for Detection of Zika, Chikungunya, and Dengue Viruses. *Emerg Infect Dis* **22**, 1295–1297 (2016).
51. Gordon, A. *et al.* Prior dengue virus infection and risk of Zika: A pediatric cohort in Nicaragua. *PLoS Med* **16**, e1002726 (2019).
52. Cohen, J. *Statistical Power Analysis for the Behavioral Sciences*. (Lawrence Erlbaum Associates, 2013).
53. Johnson, B. W., Russell, B. J. & Lanciotti, R. S. Serotype-Specific Detection of Dengue Viruses in a Fourplex Real-Time Reverse Transcriptase PCR Assay. *J Clin Microbiol* **43**, 4977–4983 (2005).
54. Dias, A. G. *et al.* Complement-dependent virion lysis mediated by dengue-Zika virus cross-reactive antibodies correlates with protection from severe dengue disease. *Cell Rep* In Press (2025).
55. Kudlacek, S. T. *et al.* Designed, highly expressing, thermostable dengue virus 2 envelope protein dimers elicit quaternary epitope antibodies. *Sci Adv* **7**, 4084–4099 (2021).

Acknowledgments: We thank the study personnel at the Centro de Salud Sócrates Flores Vivas, the Nicaraguan National Virology Laboratory, the Hospital Infantil Manuel de Jesús Rivera, and the Sustainable Sciences Institute in Nicaragua. We are particularly grateful to the study participants and their families. We would also like to thank Olivia Cuaresma for her technical support and Dr. Jeffrey R. Strich and Kiana Allen for their contributions to prior development of the NETosis assay.

Funding: This work was supported by NIH/NIAID grants P01AI106695 (EH) and U01AI153416 (EH). The Nicaraguan cohort and hospital studies were supported by NIH/NIAID grants U19AI118610 (EH), R01 AI099631 (AB), P01AI106695 (EH), and U01AI153416 (EH). MJRB is supported by funding from the Research Centers in Minority Institutions (RCMI) Center for Research Resources Grant and the Molecular and Genomics Core (U54MD007579) and the Hispanic Alliance for Clinical and Translational Research - Mentor Mentee Program Grant (5U54GM133807-03)

Author contributions:

Conceptualization: JACO, EH

Methodology: JACO, EH, SB, JVZ, VR, BB, MJRB, GA

Investigation: JACO, ED, AB, DEMJ, VR, BB, JZ, JH, AGD

Visualization: JACO

Funding acquisition: EH, GA, MJRB

Project administration: EH

Supervision: EH

Writing – original draft: JACO, EH

Writing – review & editing: JACO, EH, SB, JVZ, AGD, VR, BB, MJRB, DEMJ, GA, JZ, JH

Competing interests: EH laboratory received research funds from Takeda Vaccines Inc. to test samples from vaccine recipients. EH served on one-time advisory boards for Merck and Takeda. G.A. was an employee of Moderna Therapeutics and holds equity in Leyden Labs and Systems Seromyx. The other authors declare that they have no competing interests.

Data and materials availability: All data associated with this study are present in the main text or supplementary materials. The associated code is available for reference on Zenodo. Reference code and datasets for antibody profiling and coefficient adjustment using regularization (DOI: 10.5281/zenodo.14837883), reference code for assessing the classification performance of IgA, IgG, and IgG/IgA avidity (DOI: 10.5281/zenodo.14837889), and source data for figures (DOI: 10.5281/zenodo.14837915). After securing approval from the UC Berkeley Committee for the Protection of Human Subjects, individual data for figure reproduction can be shared with external researchers. For data access arrangements, please contact E.H. at eharris@berkeley.edu. Standard data and material transfer agreements govern all data used in this study.

Supplementary Materials

Figs. S1 to S3

Table S1

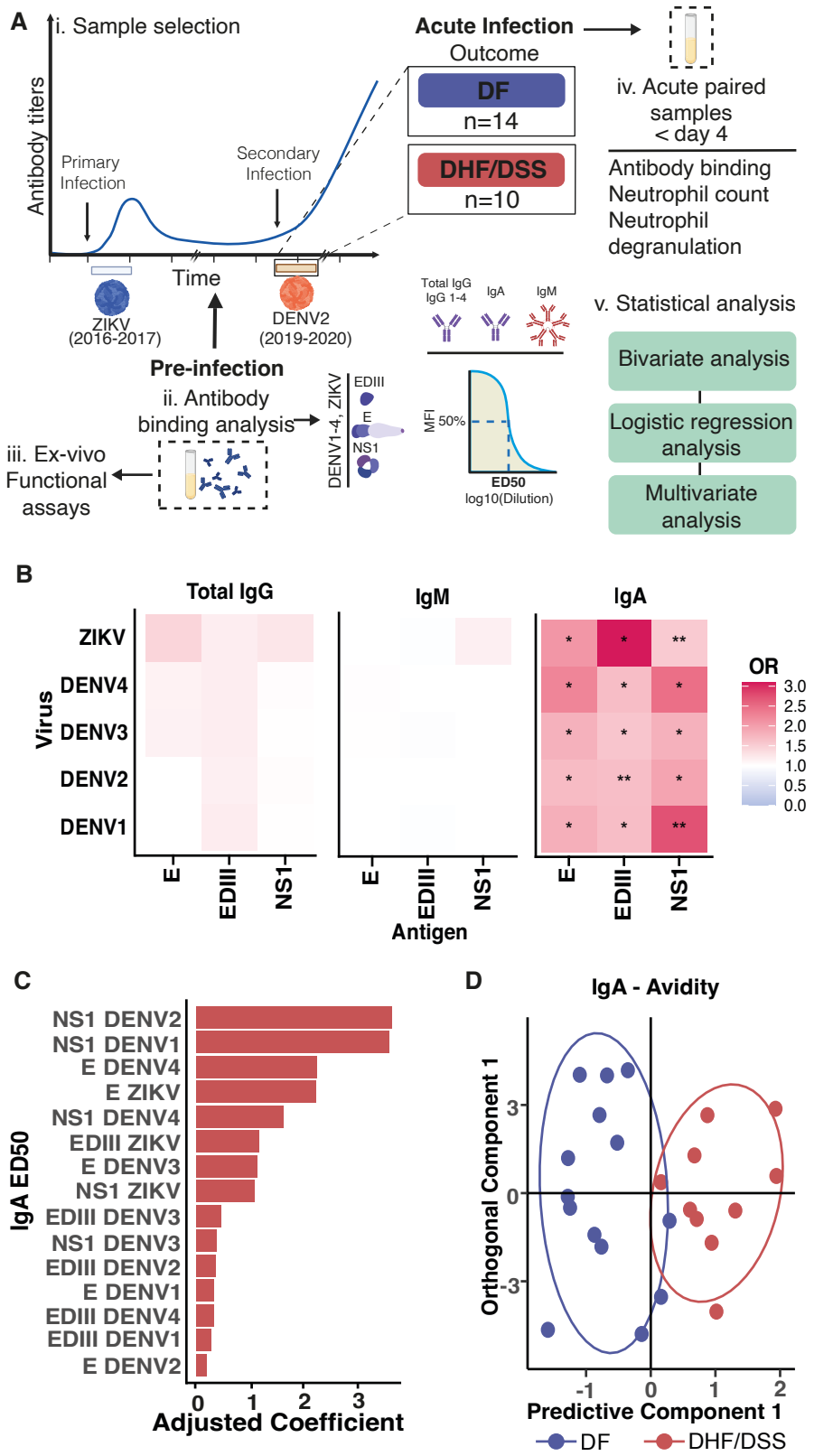

Fig 1. Study design and antibody profiling of post-ZIKV DENV2 cases in the Pediatric Dengue Cohort Study. (**A**) Study workflow. (i) Sample selection: serum samples from children

with primary ZIKV infection (2016) who developed dengue fever (DF, n=14) or dengue hemorrhagic fever/dengue shock syndrome (DHF/DSS, n=10) during a subsequent DENV2 infection (2019–2020) were analyzed. (ii) Antibody binding analysis was performed in pre-infection samples (after the primary ZIKV infection and before the subsequent DENV2 infection). (iii) *Ex vivo* functional assays with pre-infection antibodies were performed to analyze neutrophil activation, and (iv) neutrophil involvement during acute infection was assessed using paired acute-phase samples. (v) The statistical approach involved bivariate and multivariate analysis. (**B**) Heatmaps display the odds ratio of developing DHF/DSS for IgG, IgM, and IgA binding to the antigens tested. Significance: *p<0.05, **p<0.01 after False Discovery Rate (FDR) correction. (**C**) Adjusted coefficients via regularization reveal NS1 DENV2 binding as the strongest predictor of disease severity. (**D**) Total IgA avidity discriminates DF and DHF/DSS cases, shown by Orthogonal Partial Least Squares Discriminant Analysis (OPLS-DA; Accuracy=0.92, [95% CI=0.62–1], p=0.015, R2Y=0.715, Q2=0.473). Blue dots: DF; red dots: DHF/DSS.

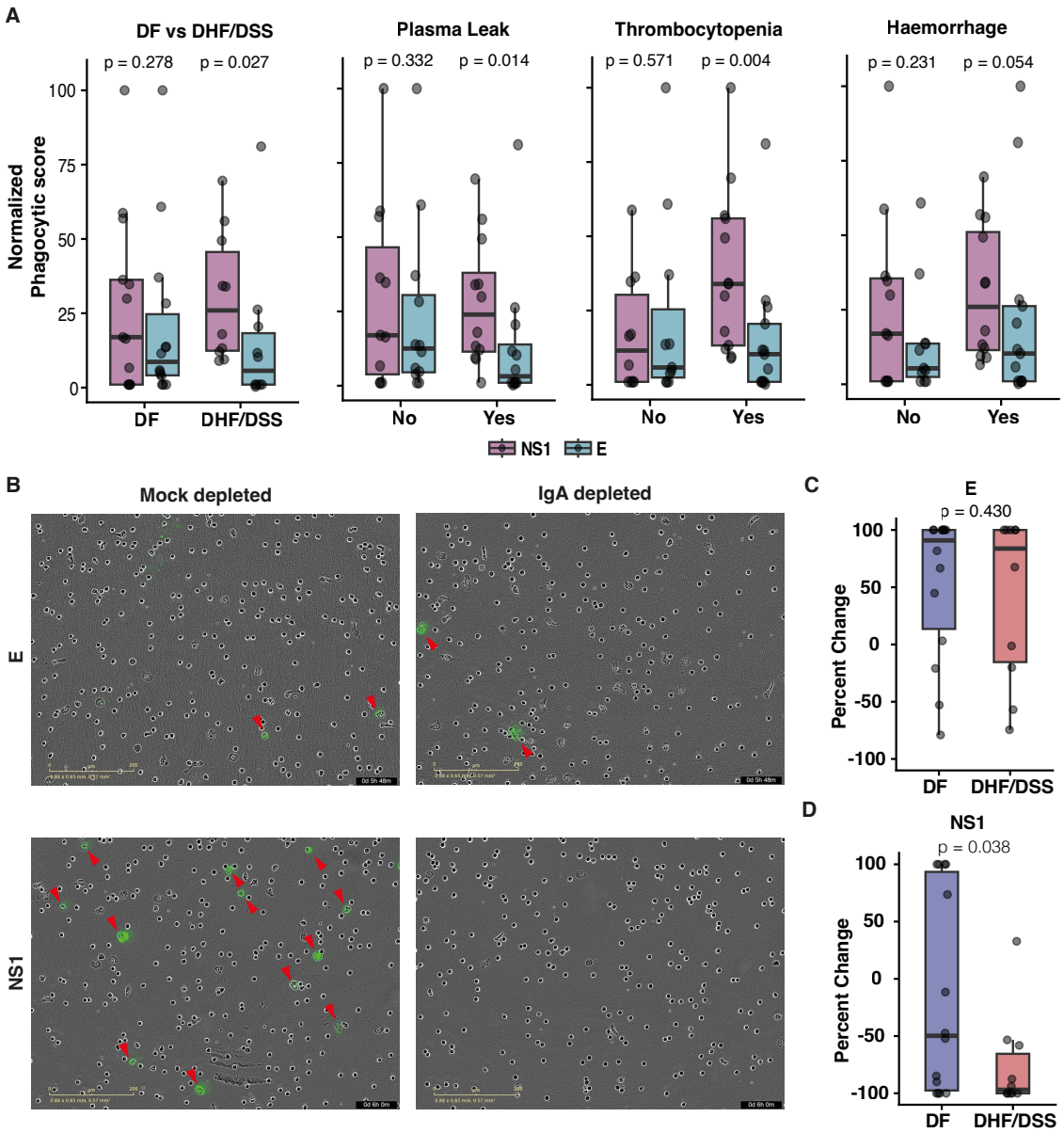

Fig. 2. IgA antibodies targeting NS1 induce enhanced neutrophil activation in DHF/DSS cases. (**A**) Antibody-dependent neutrophil phagocytosis (ADNP) normalized phagocytic scores across clinical groups and severe disease manifestations. Data points represent the average of two replicates from two different healthy donors per sample (DF=14, DHF/DSS=10). Children with DHF/DSS exhibited significantly higher ADNP against NS1 compared to E, particularly in association with plasma leakage (p=0.014) and thrombocytopenia (p=0.004). The data indicate a skewed neutrophil activation response toward NS1 in severe cases. (**B**) Representative microscopy images of NETosis assays. Panels compare mock-depleted plasma (left) and IgA-depleted plasma (right) for E and NS1 antigens. IgA depletion significantly reduces NET formation in NS1-coated wells (p=0.038), highlighting the role of IgA in mediating neutrophil activation. Red arrows

indicate NETs. Scale bar=200 µm. (**C**, **D**) Quantification of percent change in NETosis signal for E (**C**) and NS1 (**D**) antigens after IgA depletion. Data points represent the percent change comparing paired depleted and mock-depleted samples from participants who developed DF (n=14) or DHF/DSS (n=10). While no significant difference was observed for E, NETosis was significantly reduced in DHF/DSS cases when NS1-specific IgA was depleted.

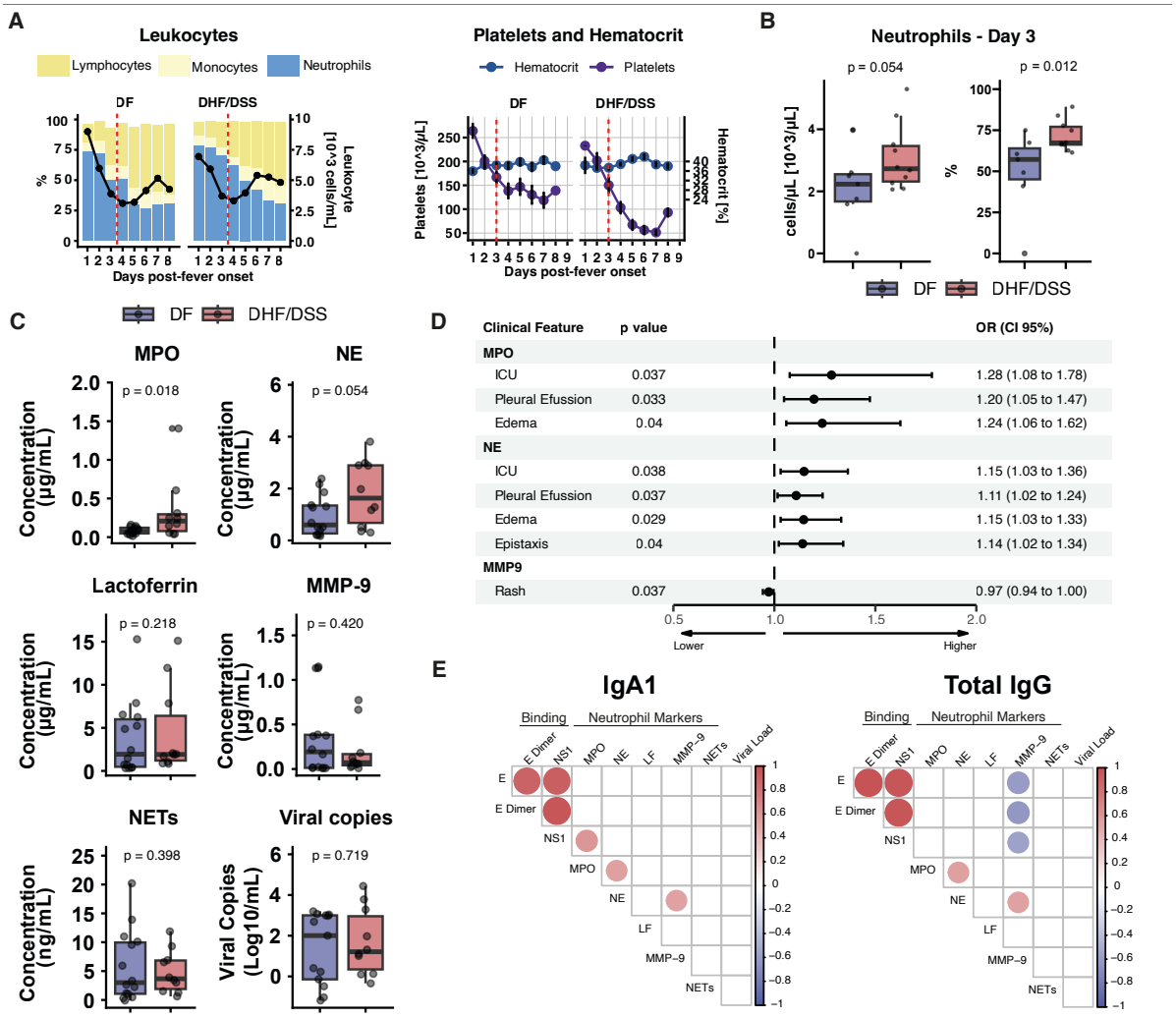

Fig 3. Enhanced neutrophil activation during acute infection correlates with disease severity and binding of anti-NS1 IgA1 antibodies. (**A**) Relative leukocyte proportions, platelet counts, and hematocrit levels in DF and DHF/DSS cases over time. Day 3 post-fever onset is marked with a dashed red line. (**B**) Neutrophil counts on day 3 post-fever onset—prior to the onset of thrombocytopenia (platelet count<100,000/µL)—were significantly elevated in children who progressed to DHF/DSS (p=0.012). (**C**) Levels of primary granule markers (myeloperoxidase [MPO], neutrophil elastase [NE]), secondary granule markers (lactoferrin), tertiary granule markers (MMP-9), NETs, and viral loads among children with DF or DHF/DSS. DHF/DSS cases displayed higher levels of MPO (p=0.018) and NE (p=0.054), with no significant difference in viral load. (**D**) Logistic regression shows significant correlation between MPO, NE, and severe outcomes such as ICU admission and pleural effusion (OR with 95% CI). (**E**) Correlation heatmaps between antibody binding and neutrophil degranulation. Only significant correlations (adjusted p-

value<0.05) after FDR correction are displayed. IgA1 binding to NS1 positively correlates with MPO and NE, while IgG inversely correlates, highlighting distinct antibody roles in neutrophil activation.

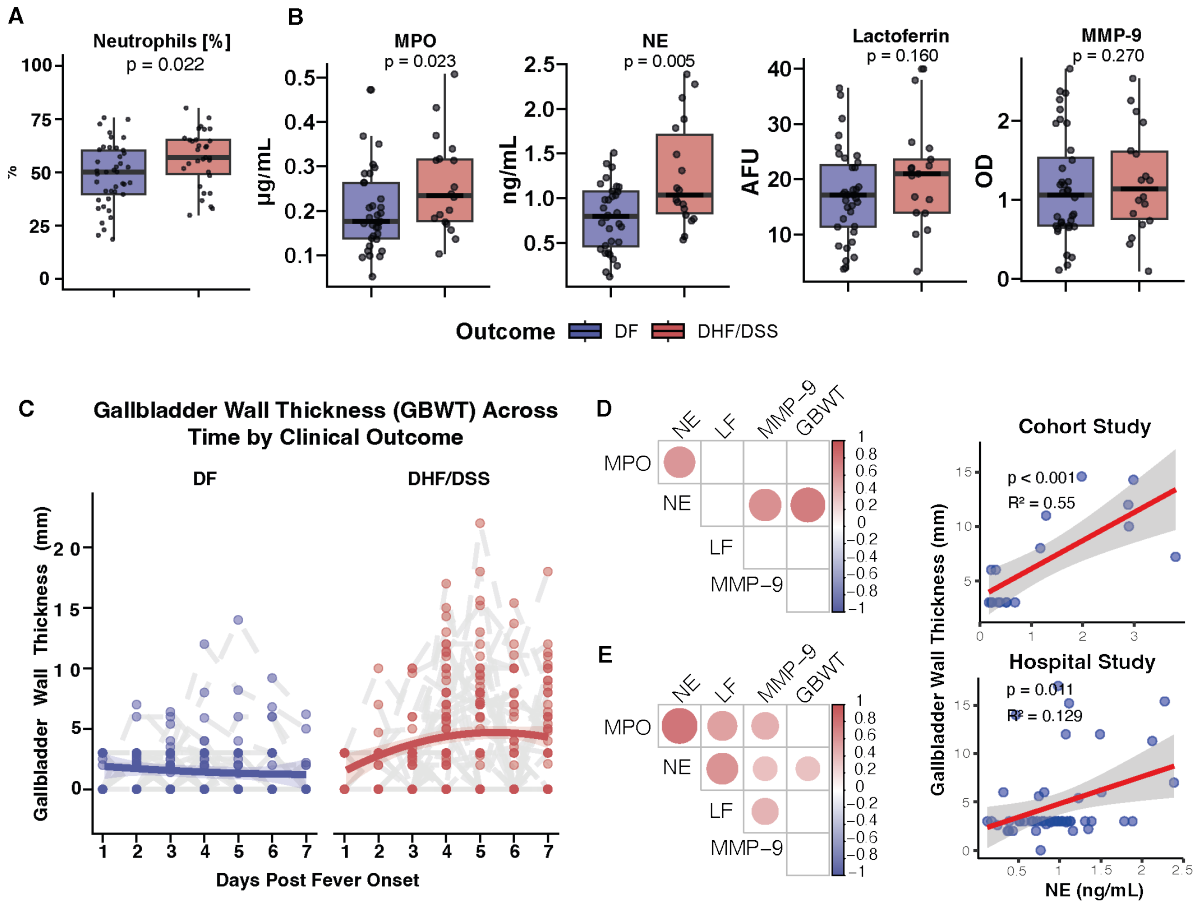

Fig. 4. Neutrophil activation precedes and correlates with vascular leakage during acute dengue infection across two independent studies. (**A**) Relative neutrophil count in DF or DHF/DSS cases in the Pediatric Dengue Hospital Study (PDHS). Consistent with findings from the Pediatric Dengue Cohort Study (PDCS), DHF/DSS cases had significantly higher relative neutrophil count compared to DF cases (p=0.022). (**B**) Levels of neutrophil degranulation markers, (myeloperoxidase [MPO], neutrophil elastase [NE], lactoferrin [LF], and matrix metalloproteinase-9 [MMP-9]) in DHF/DSS vs. DF cases. DHF/DSS cases in the PDHS showed significantly elevated MPO (p=0.023) and NE (p=0.005) levels. AFU: Arbitrary fluorescent units, OD: Optical density. Data points represent the average of two technical replicates from DF (n=36) or DHF/DSS (n=18) cases. Outliers were excluded from analysis. (**C**) Gallbladder wall thickness (GBWT) over time in DF and DHF/DSS cases in the PDHS and PDCS. Greater gallbladder wall thickeness was observed in DHF/DSS cases during acute infection, reflecting increased vascular leakage. (**D**, **E**) Correlation analyses between neutrophil degranulation and gallbladder thickness in the PDCS (**D**) and PDHS (**E**). A positive correlation is observed between NE levels (measured

on/before day 3 post-fever onset) and maximum gallbladder wall thickness in the PDCS ($p<0.001$, $R^2=0.35$) and PDHS ($p=0.01$, $R^2=0.128$).